

2004

46. Jahrgang

22. November 2003, Herausgeber: Prof. Dr.-Ing. H. P. Krause, Institut für Materialprüfung, Universität Regensburg, 93040 Regensburg, Tel.: 0941/943-2450, Fax: 0941/943-2451, E-Mail: h.p.krause@fz-juelich.de

22. November 2003, Herausgeber: Prof. Dr.-Ing. H. P. Krause, Institut für Materialprüfung, Universität Regensburg, 93040 Regensburg, Tel.: 0941/943-2450, Fax: 0941/943-2451, E-Mail: h.p.krause@fz-juelich.de

Verlag Hanser Verlag München, 8053 Regensburg, Tel.: 0941/943-2450, Fax: 0941/943-2451, E-Mail: h.p.krause@fz-juelich.de

www.hanser.de/mp

Organ der
Bundesanstalt für
Materialforschung
und -prüfung
Berlin (BAM)

MATERIALS
TESTING

MATERIALPRÜFUNG

Werkstoffe und Bauteile,
Technologien und Anwendungen

Praxishandbuch – Metallbauherhandwerk, Konstruktionstechnik

Praktische Bau- und technische Regeln

Band 1: Praxishandbuch DIN EN 1025, 45. Auflage, 2003, 978-3-446-15371-6

Die ersten Praktischen Handbücher des Stahlbaus erschienen im Jahr 1900 unter dem Titel „Handbuch der Eisen- und Stahlbau-Arbeiten“.

Die ersten „Praktischen Metallbauhandbücher“ wurden im sog. „Metallbauhandbuch“ zwischen 1923 und 1928 erarbeitet und mit Grundlagen und Anwendungen für den Bau von Stahlbauten ausgestattet. Die frühen Praktischen Handbücher waren überwiegend auf die Anwendung von Stahl- und Ausbauteilen ausgerichtet. Ab 1960 begann die Entwicklung der Stahlbauhandbücher zur heutigen Form.

Alle Rechte, auch die des Nachdrucks, der photomechanischen Wiedergabe dieses Sonderdrucks und der Übersetzung, behält sich der Verlag vor.

Carl Hanser Verlag
München

Jahre 45 (2004) 7-8

Autoren-Fortdruck

Die Autoren-Fortdrücke sind ein neues Praktischhandbuch „Metallbauherhandwerk, Konstruktionstechnik“ empfohlen. Dient Fachgenossen der weiteren Fortbildung als Band 2 der Reihe „DIN-Normen für das Handwerk“ als Begriff. Aufbauend auf diesem Standardwerk umfasst das aktuelle Fortdrückband die wichtigsten DIN-, DIN-RN- und DIN/ISO-Normen zu folgenden Gebieten:

- Metallische Werkstoffe (Technische Anforderungsprofile, Anwendung)
- Korrosionsschutz (Beschichtungsverfahren, Reaktivverzinken),
- schweißtechnische Allgemeinanforderungen an Schweißverbindungen, Schweißverfahren für metallische Werkstoffe, Lötvergussverfahren (Lötprofile)
- Fugen, Flansche, Treppen, Anordnungen von Verklebungen, Luftdurchlässigkeit, Widerstand gegen Windlast, Einbaureihenfolge,

Die Autoren-Fortdrücke sind ein neues Praktischhandbuch „Metallbauherhandwerk, Konstruktionstechnik“ empfohlen.

• Decken- und Außenwandschalldämmung,

• Türen und Fenster,

Das Rahmenprogramm für den Nachdruck führt die drei neu überarbeiteten Allgemeinen Technischen Verordnungen (ATV) aus dem Teil 2 der VOB-Vorlage und Verordnung für Bauleistungen 2002:

- ATV DIN 18331 „Stahlbauarten“
- ATV DIN 18330 „Metallbauarbeiten“
- ATV DIN 18336 „Verklebungsarbeiten“

Alle Dokumente legen die Anwendungsbereiche fest, die bezüglich der Bauart, Art und Stufe der Ausführung, der Klemp- und Schweißarbeiten sowie der Absicherung z.B. Gewölbe gelten.

Vom Praktizieren bis Praktizierend ausgestattet, wird auch dieses Normen-Kompendium allen Metallverarbeitenden Betrieben bei der Bewältigung der täglichen Arbeit hilfreich zur Seite stehen.

Thermal fatigue life prediction

Verification of Coffin-Mansons's law in the phase transformation range of ferrite matrix ductile cast iron

Morihito Hayashi, Kanagawa,
Japan

For clarifying the behavior of thermal fatigue and verifying the role of Coffin-Manson's law in thermal fatigue, out-of phase type thermal fatigue tests were carried out on ferritic ductile cast iron. As a result of the tests, the dependence of thermal fatigue life and the plastic strain produced in each cycle on cyclic peak temperature and the dependence of thermal fatigue life on cyclic plastic strain were made clear. Particularly, the exponent and the coefficient in the latter relationship, i.e. Coffin-Manson's law, are kept constant over all ranges, including the phase transformation range. And it shows that the thermal fatigue life can be predicted by tensile the properties of specimens at room temperature. By the way, the microstructure and the fracture surface of failed specimens were observed and the mechanism of thermal fatigue is discussed here.

Because of its superior mechanical properties and its low price, ductile cast iron is utilized widely as a leading industrial material. And several studies on its strength at elevated temperature were reported [1,2,3,4,5,6]. In the former report [7] on thermal fatigue, two kinds of serration in cyclic thermal stress, visual crack on specimens and the effect of cyclic peak temperature on the fatigue life were introduced. In the study, continuing a former report, the effects of cyclic peak temperature on

fatigue life, repeated cyclic test temperature on it, plastic strain produced in each thermal cycle, and the relationship between thermal fatigue life and cyclic plastic strain around the $\alpha \leftrightarrow \gamma$ phase transformation are investigated and discussed here.

Materials and Experimental Procedure

The material and experimental procedure are as reported in the former [7].

The thermal fatigue tests were carried out on spheroidal graphite cast iron with ferrite matrix, classified as FCD400 in JIS. In the test, the thermal cycle was given repeatedly from the temperature 323K to the peak temperature which was selected as a parameter from 673K to 1273K at constant rate of 3.1K/s with the form of a triangular thermal cycle to the specimen. The diameter of the specimen is 10 mm and its gauge length is 15 mm, which is constrained axially completely so the displacement

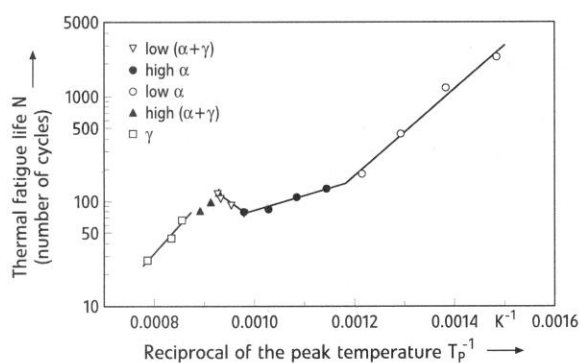


Figure 1. The diagram of thermal fatigue life versus the reciprocal of cyclic peak temperature of thermal fatigue on ferritic ductile cast iron

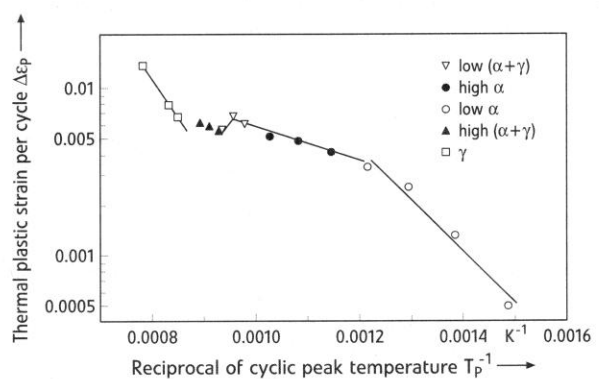


Figure 2. The diagram of thermal plastic strain per cycle versus the reciprocal of cyclic peak temperature of thermal fatigue on ferritic ductile cast iron

of the gauge length is always kept zero during the test. And the thermal fatigue life N was determined by the number of thermal cycles to failure in each test.

Experimental results and discussion

Fatigue life versus Cyclic peak temperature. The relation of thermal fatigue life N to the cyclic peak temperature T_p is obtained as shown in Fig. 1, which can be divided roughly into 3 ranges. In the first range from 673K to 1023K, the fatigue life decreases with the increase of cyclic peak temperature. In the second range from 1023K to 1078K, the cyclic life increases with the increase of peak temperature. And in the third range above 1078K, which is like the first range, the life decreases with the increase of the cyclic peak temperature. The first range, furthermore, can be divided into two sub-ranges, from 673K to 823K and from 823K to 1023K, respectively, where the slope of the curves is different from each other. And the third range also can be divided into two sub-ranges, from 1078K to 1123K and from 1123K to 1273K. The relationships over all ranges can be expressed in an Arrhenius equation (1),

$$N = A_N \cdot \exp(Q_N/RT_p) \quad (1)$$

N : thermal fatigue life, R : gas constant, 8.31451 J/mol·K, Q_N : thermal activation energy for thermal fatigue life, kJ/mol, and A_N : coefficient. The data Q_N and A_N for each range are as shown in Tab. 1.

Cyclic thermal plastic strain versus cyclic peak temperature. The cyclic thermal plastic strain $\Delta\epsilon_p$ is attained by the difference of thermal expansion between two points where thermal stress vanishes to zero in each thermal cycle. Then the diagram of $\Delta\epsilon_p$ versus T_p was obtained as shown in Fig. 2, the relationship can be divided also into five divisions as described above and can be expressed as in the equation (2),

$$\Delta\epsilon_p = A_p \cdot \exp(Q_p/RT_p) \quad (2)$$

Q_p : thermal activation energy for $\Delta\epsilon_p$, and A_p : the coefficient, as shown in Tab. 2.

Comparing activation energies, Q_N and Q_p are about one third or one fourth of that for self-diffusion and near that of

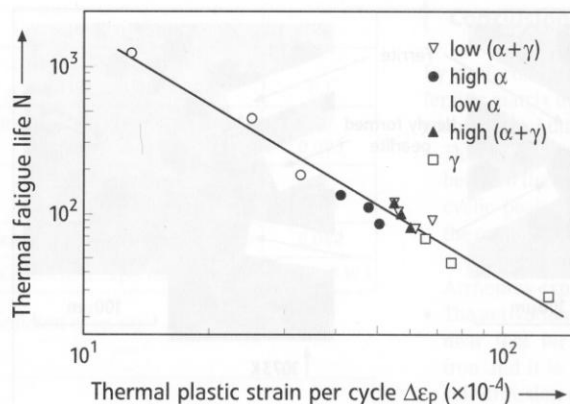


Figure 3. The diagram of thermal fatigue life versus thermal plastic strain per cycle

carbon and tensile strength as shown in Tab. 3 [1,8,14].

Thermal fatigue life versus plastic strain per cycle. As for the diagram of fatigue life versus plastic strain per cycle as shown in Fig. 3, the larger the plastic strain is, the lower the fatigue life is and the relation can be expressed roughly by a straight line in full logarithmic scale all over the temperature ranges by the equation (3) in a single power function with a coefficient and an exponent for over all ranges, in this case, κ_p : 0.59 and C_p : 0.082. These are 0.57-0.62 and 0.023-0.192 for FCD450 in α range [6].

$$\Delta\epsilon_p \cdot N^{k_p} = C_p \quad (3)$$

Change of microstructure around transformation range on thermal fatigue. As shown in Fig. 4, when the cyclic peak temperature is over 1023K and reaches 1098, carbon atoms start to flow out from the spheroidal graphite, along the boundaries and diffuse into the ferrite inner grains, which were transformed into austenite, and then precipitated into pearlite while cooling process. While the peak temperature approaches 1173K, the flowed atoms of carbon near the spheroidal graphite are absorbed again back to form the structure of bull's eye. It is clear that the $\alpha \leftrightarrow \gamma$ transformation takes place at the temperature within the range from 1023K to 1173K in the thermal fatigue test.

Temperature range	673K-823K	873K-1023K	673K-1023K	1023K-1078K	1078K-1123K	1078K-1273K	1173K-1273K
Q_N in kJ/mol	79.5	26.5	58	- 60.8	88.5	84.1	104
A_N	1.85×10^{-3}	3.42	0.055	9.87×10^{-4}	0.0062	0.0102	0.0014

Table 1. Activation energies and coefficients for each range in equation (1)

Temperature range	673K-823K	873K-1023K	673K-1023K	1023K-1078K	1078K-1123K	1078K-1273K	1173K-1273K
Q_p in kJ/mol	- 58.8	- 19.2	- 38.1	24.3	- 19.6	- 47.1	- 85.9
A_p	20.6	0.0578	0.666	3.76×10^{-4}	0.0485	0.956	41.9

Table 2. Activation energies and coefficients of the equation (2) for each range

Matrix	Activation energy in kJ/mol						
	Self-diffusion	Grain boundary	Diffusion of carbon	Q_N	$- Q_p$	Tensile strength	Tensile deform.
in α	251-264		80	26.5-79.5	19.2-58.8	60.7	357
in γ	234-310	159	148	104	85.9	58.7	313

Table 3. Activation energies for ductile cast iron

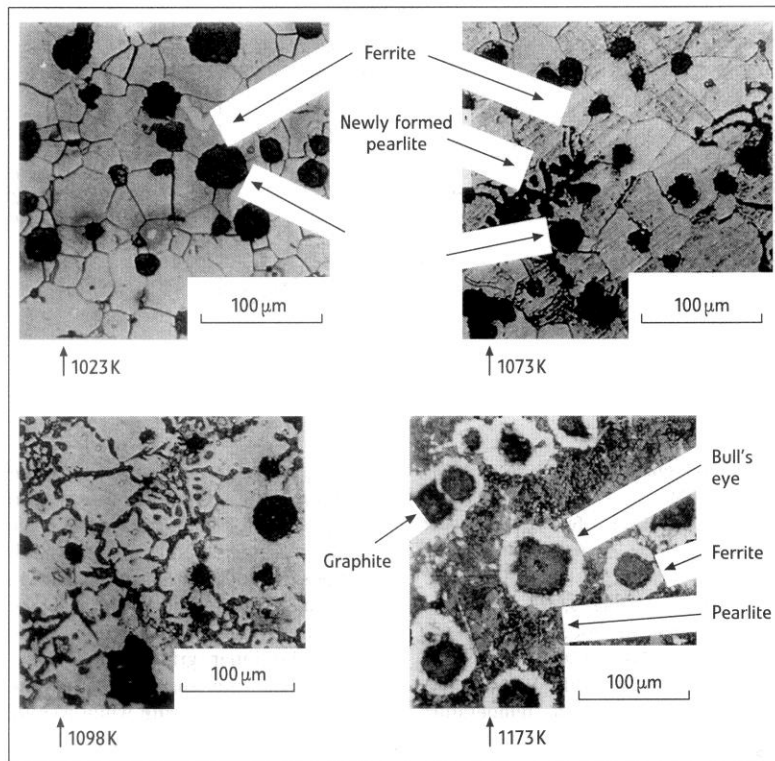


Figure 4. Microstructure changed with different peak temperature around $\alpha \leftrightarrow \gamma$ transformation

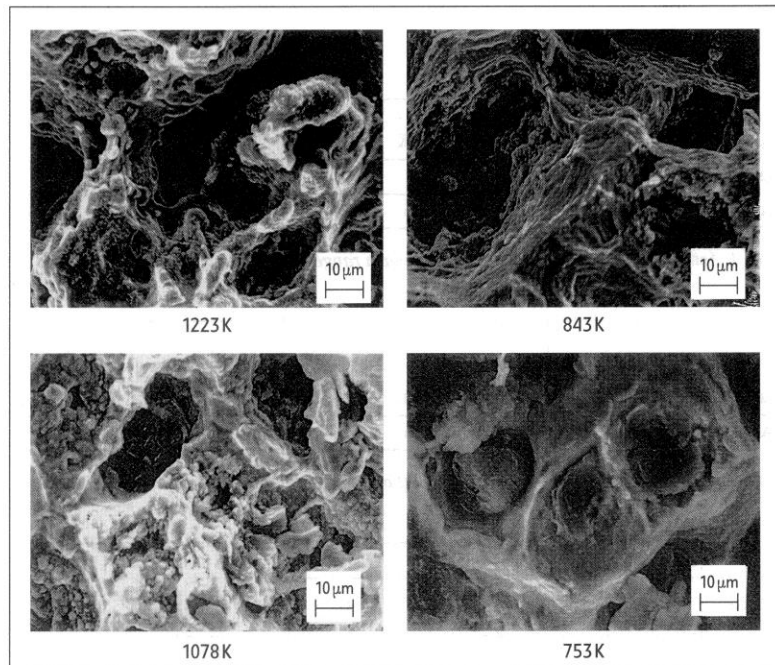


Figure 5. SEM pictures of fracture surface at different cyclic peak temperatures of thermal fatigue test on ductile cast iron

Fractography on thermal fatigue. Thermal fatigue fracture around the phase transformation range is as shown in Fig. 5. In the peak temperature range of 673K-1023K, there are two kinds of plastic fracture pattern caused by a great deformation of ferrite matrix around nodular graphite: one is trans-granular plastic fracture at lower α temperature range presented by the picture at 753K, and the other one is inter-granular plastic fracture at higher α temperature range by that at 843K which is effected by the weakening of grain boundary at elevated temperature. From 1073K to 1123K, as the picture at 1078K, it shows the fracture of coexistence of α and pearlite transformed from γ matrix during the cyclic cooling process. And at 1223K, it shows the fracture of pearlite matrix transformed from austenite.

Comparison with Coffin-Manson's law. As for the equation (3) related to N and $\Delta\varepsilon_p$, it is the same as the Coffin Manson's model [9,10,11,13], in which the exponent κ_p is 0.5 proposed by Coffin [9] and 0.6 or 0.5 - 0.7 by Manson [12]. These values are near the experimental value of 0.59 attained here. As to C_p , it is 0.1 calculated from the tensile elongation ε_T of 20% as ε_f , and it also shows 0.093 calculated from the rate of reduction ϕ of 17% by the equation (4) suggested by Coffin, and furthermore, it shows 0.06 calculated by the equation (5) proposed by Manson, and these are near the experimental value of 0.082 obtained here.

$$C_p = \varepsilon_f / 2 = (\%) \ln (100 / (100 - \phi)) \quad (4)$$

$$C_p (\%) = (\varepsilon_f (\%))^{0.6} \quad (5)$$

These data as shown in Tab. 4 suggest the thermal fatigue life can be predicted at least roughly by the tensile test data at room temperature.

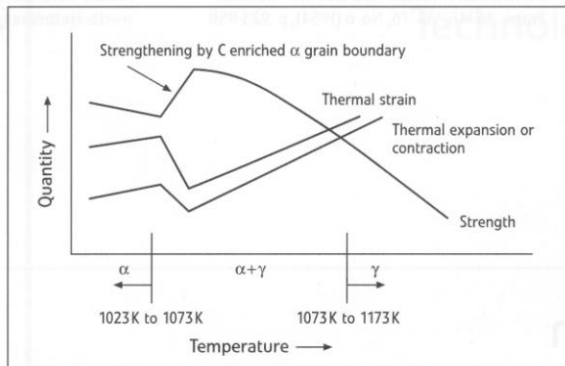
Discussion of cyclic elementary process in phase transformation

In the transformation range from 1023K to 1173K, the plastic strain decreases and the fatigue life increases with the increase of the peak temperature from 1023K to 1073K that is basically as shown in Fig. 6 caused by the relaxing of thermal expansion through the matrix contracting due to phase transformation [13] from ferrite into austenite and by strengthening of the carbon-enriched

	κ_p		C_p
Coffin [9]	0.5	by the eq. (4) as $\varepsilon_f = \varepsilon_T$ from elongation of 20%	0.1
		by the eq. (4) from the rate of reduction of 17%	0.093
Manson [12]	0.6 or 0.5–0.7	by the eq. (5) as $\varepsilon_f = \varepsilon_T$ from elongation of 20%	0.06
experimental value in the study	0.59	experimental value in the study	0.082
FCD450 in α experimentally [6]	0.57–0.62	FCD450 in α experimentally [6]	0.023–0.192

Table 4. Discussion about the exponent and the coefficient of eq. (3)

Figure 6. Phase Transformation Effect



grain boundaries which are to be precipitated into pearlite at cooling process in each cycle. Once the pearlite precipitates along the grain boundary and spreads further into the inner grain, the plastic strain starts to increase again as the repeated peak temperature increases, so the fatigue life decreases again simultaneously. Here the behaviors and properties of α grain boundary are considered as follows. If phase transformation is proceeding gradually, then α (ferrite) \rightarrow γ (austenite) transformation takes place at first in the grain boundary at heating process, then the body centered cubic (bcc) structure transforms into the face centered cubic (fcc) structure. Then, due to the different density in both of them, it causes tension along the fcc boundary and compression in the inner bcc grain. Carbon atoms are absorbed from the graphite nodule and flow into and along the fcc grain boundary. So, the diffusion of carbon strengthens the weakened α grain boundary to obstruct boundary deformation to make both the grain boundary and the inner grain homogeneous in strength and fluidity to disperse defect formation and avoid a concentration of defects. On the other hand, the contracting of γ relaxes its thermal stress, which lessens defects

or damages, to strengthen the matrix more while it is precipitated into pearlite. However, while phase transformation advances further, the above-described effect disappears and the fatigue life decreases with the increase of repeated temperature.

Summary

Verifikation des Coffin-Manson Gesetzes im Gebiet der Phasentransformation ferritischen Gusseisens. Um das Verhalten bei thermischer Ermüdungsbeanspruchung zu klären und um das Coffin-Manson Gesetz zu verifizieren, wurden thermale Ermüdungsversuche mit ferritischen Gusseisen durchgeführt. Als Ergebnisse dieser Tests wurden die Abhängigkeit der thermischen Ermüdfestigkeit und der plastischen Dehnung innerhalb jeden Lastwechsels von der zyklischen Spitzentemperatur sowie die Abhängigkeit der thermischen Ermüdfestigkeit von der zyklischen plastischen Dehnung geklärt. Insbesondere wurden der Exponent und der Koeffizient im Coffin-Manson Gesetz über alle Bereiche, einschließlich der der Phasentransformation, konstant gehalten. Es stellte sich heraus, dass die thermische Ermüdfestigkeit anhand der Festigkeitseigenschaften bei Raumtemperatur vorausgesagt werden kann. Darüber hinaus wurden die Gefüge und die Bruchoberfläche der Proben untersucht und es wird der Mechanismus der thermischen Ermüdung diskutiert.

Conclusions

By performing thermal fatigue tests on ferritic matrix ductile cast iron, the main results are obtained as follows:

- The thermally activated relationships between the thermal fatigue life and the cyclic peak temperature and between the cyclic thermal plastic strain and the cyclic peak temperature are obtained in Arrhenius expression in all ranges.
- The activation energy for fatigue life is near that for diffusion of carbon in iron and it is about $\frac{1}{2}$ or $\frac{1}{4}$ of that for self-diffusion of iron atoms.
- The relationship between the thermal plastic strain and the fatigue life can be expressed by the model of Coffin-Manson's law with a coefficient and an exponent, all over temperature ranges including phase transformation.
- Thermal fatigue life can be predicted by the tensile data at room temperature.
- The pattern of thermal fatigue fracture changes around the phase transformation range.
- Thermal fatigue in phase transformation is effected by the thermal contraction and the diffusion of carbon along the grain boundary.

References

- Chijiwa, K.; Hayashi, M.: Mechanical Properties of Ductile Cast Iron at Temperatures in the Region of Room Temperature to Liquidus, Journal of The Faculty of Engineer-

- ing, The University of Tokyo (B), Vol. 35, No. 2 (1979), p. 205-230
- 2 Chijiwa, K.; Hayashi, M.: Mechanical Properties of Ductile Cast Iron at Temperatures in the Region of Room Temperature to Liquidus. Imono, Vol. 51(1979), p. 395-400
- 3 Yasue, K.; Isotani, M.; Kondo, Y.; Kawamoto, N.: Thermal Fatigue of Spheroidal Graphite Cast Iron. Imono, Vol. 54 (1982), p. 739-743
- 4 Nakashiro, M.; Kitagawa, M.; Hukuhara, Y.; Oohama, S.: Thermal Fatigue and High Temperature Low Cycle Fatigue Properties of Spheroidal Graphite Cast Iron, Transaction of Iron and Steel, Vol. 70 (1984), p. 1230
- 5 Takeshige, N.; Uosaki, Y.; Asai, H.: Thermal Fatigue Behavior of Heat Resistant Cast Iron for Automobile, Prepr. of Jpn. Soc. Mech. Eng. No. 940-10 (1994), p. 56-58
- 6 Yasue, K.; Mtsubara, H.; Isotani, M.; Kondo, Y.: Temperature Dependence of Low Cycle Fatigue Life in Cast Iron. Imono, Vol. 52 (1980), p. 669-674
- 7 Hayashi, M.: Features on Thermal Fatigue of Ferrite Matrix Ductile Cast Iron, in: K.T. Rie and P.D. Portella (ed.), Low Cycle Fatigue and Elasto-Plastic Behaviour of Materials, Oxford Elsevier Science Ltd (1998), p. 161-166
- 8 HumeRothery, W.: The Structure of Alloys of Iron, Pergamon Press (1966)
- 9 Coffin, L.F. Jr.: A Study of the Effects of Cyclic Thermal Stresses on a Ductile Material, Trans. ASME, Vol. 76, No. 6 (1954), p. 923-950
- 10 Coffin, L.F.Jr.; Tavarnelli, J.F.: Cyclic Straining and Fatigue of Metals, Trans. Met. Soc. AIME, Vol.215, No.5 (1959), p. 794-807
- 11 Manson, S.S.: Behavior of Materials under Conditions of Thermal Stress, NACA Tech. Note, 2933 (1954)
- 12 Manson, S.S.: Fatigue: A Complex Subject - Some Simple Approximations, Exper. Mechanics, Vol. 5, No. 7 (1965), p. 193-226
- 13 Manson, S.S.: Thermal Stress and Low-Cycle Fatigue. McGraw-Hill Book Co., New York (1966)
- 14 Brandes, E. A.; Brook, G. B.: Simthells Metals Reference Book, 7th ed. Butterworth-Heinemann, Oxford, (1992)

Schneller Wuchten

Die „BTD-UNI 44“, eine neue Generation von Steuerungen für Industrie-Auswuchtmaschinen von Schmitt Europa, Pfungstadt, verbindet große Präzision mit hoher Wiederholbarkeit. Sie sollen einen erhöhten Durchsatz bei Auswuchtmaschinen ermöglichen.

Die Steuerung arbeitet mit Sinuswellen-Demodulation und neuester Windows-basierter Touch-Screen-Technik und ist sowohl für statische als auch dynamische Anwendungen geeignet. Sie kann auch zum Bestimmen des Massenträgheitsmoments bei speziellen Anwendungen, wie zum Beispiel für Satelliten eingesetzt werden. Das System ist für High- und Low-Speed-Auswuchtmaschinen in horizontaler und vertikaler Bauweise konstruiert. Es arbeitet sowohl an Weich- als auch an Hartlagermaschinen mit Bauteilmassen von einigen Gramm bis zu mehreren Tonnen. Die Elektronik verfügt über einen Vier-Kanal-Eingang, so dass exakte Auswuchtungen von komplexen Baugruppen, wie zum Beispiel Kardanwellen, möglich sind. Die Software erlaubt es dem Benutzer, die BTD-UNI 44 genau auf seine Anforderungen zu konfigurieren. Das verkürzt die Auswuchzyklen um bis zu 50 Prozent.

Der Touch-Screen und leicht nachvollziehbare Bildschirmbefehle sollen ein einfaches und intuitives Bedie-

nen gewährleisten (Bild 1). Bei der Initialisierung des Auswucht-Zyklus fährt die Steuerung das Bauteil auf eine vorgegebene Drehzahl. Die aktuellen Daten des Wuchtzustands und des Drehwinkels werden in Echtzeit graphisch dargestellt.

men ist die korrekte und tatsächliche Position auf dem Bildschirm ablesbar.

Alle Ergebnisse lassen sich als Zertifikat ausdrucken oder direkt zu einer SPS-Steuerung oder einer anderen Windows-kompatiblen Software exportie-

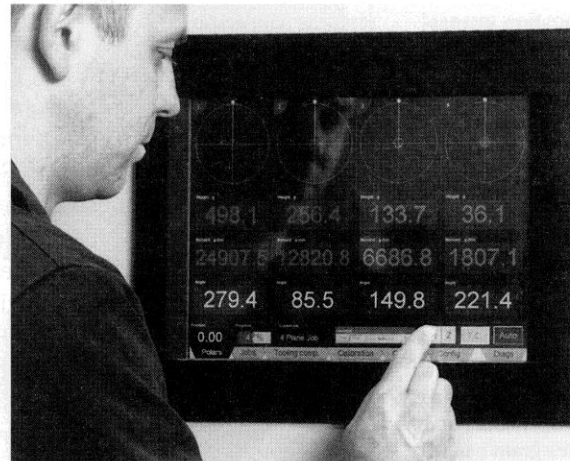


Bild 1. Der Touch-Screen ermöglicht ein einfaches und intuitives Bedienen

Die vollautomatische Version des Systems bremst das Bauteil ab, bevor es automatisch in die korrekte Position gebracht wird. Die Korrektur ist auf- oder abtragend möglich, wie zum Beispiel durch Fräsen, Bohren oder Schweißen und kann manuell, halb- oder vollautomatisch erfolgen. Bei manuellen Systemen.

Die standardmäßige Modemverbindung erlaubt eine Fernsteuerung und Ferndiagnose. Die BTD-UNI 44 wird in allen Auswuchtmaschinen der Firma Universal Balancing eingesetzt. Es besteht allerdings auch die Möglichkeit Auswuchtmaschinen anderer Anbieter damit nachzurüsten.